Research article

Identification of a novel survival and immune microenvironment related ceRNA regulatory network for hepatocellular carcinoma based on circHECTD1

Shuiqing Lan [a], Guoqiang Zhong [b],[*]

[a] *Department of Pain Management, The Affiliated Hospital of Youjiang Medical University for Nationalities, Baise, Guangxi, 533000, China*
[b] *The Graduate School, Youjiang Medical University for Nationalities, Baise, Guangxi, 533000, China*

A B S T R A C T

Background: CircHECTD1 (circ_0031450) is highly expressed in hepatocellular carcinoma (HCC) tissues and may act as an oncogene. Its specific competitive endogenous RNA (ceRNA) mechanism remains to be further elucidated.
Methods: Several databases and online platforms, including pathway activity, immune checkpoint, and overall survival analyses, were used to predict targets, download datasets, and perform online analyses. The R software was used for differential gene expression analysis, Gene Ontology (GO), Kyoto Encyclopedia of Genes and Genomes (KEGG), clinical relevance, receiver operator characteristic curve, and single-cell analysis. Cytoscape software was used to construct ceRNAs, protein-protein interactions (PPI), and pivotal networks.
Results: The ceRNA, PPI, and pivotal networks were successfully constructed. Pathway enrichment analysis was mainly related to apoptosis, cell cycle, and epithelial-mesenchymal transition (EMT) pathways. Six pivotal targets related to survival, immune infiltration, immune checkpoints, clinical stage, and diagnosis of patients with HCC were identified. The recovery function and pathway enrichment results were consistent with previous results. Single-cell analysis suggested that the pivotal targets were highly expressed in T cells.
Conclusion: We successfully constructed a prognosis and immune microenvironment-related ceRNA network based on circHECTD1, providing new insights for diagnosing and treating HCC.

1. Introduction

Hepatocellular carcinoma (HCC) is among the cancers with high incidence and mortality rates, especially in Asia. The newly diagnosed cases and deaths are predicted to continue rising over the next two decades [1]. Despite the advancements in HCC diagnosis, treatment, and prevention, the prognosis of patients with advanced HCC remains poor [2–4]. Consequently, further research on diagnosing and treating HCC remains required. Recently, non-coding RNAs (ncRNAs) have become a prominent subject in tumor research. Circular RNA (circRNA) is a member of the ncRNA family. Although it was first discovered decades ago [5], research on its functions and regulatory roles in tumors and other diseases is ongoing. MicroRNAs (miRNA) also belong to ncRNA, which can act as an epigenetic regulator that regulates tumor occurrence and progression [6–8].

---

* Corresponding author.
   E-mail address: zhong_guoqiang177@126.com (G. Zhong).

The competitive endogenous RNA (ceRNA) network was first proposed by Professor Pierpaolo Pandolfi in 2011 [9]. This process has recently become a novel regulatory mechanism for tumor development. This network involves interactions between coding RNAs (mRNAs) and ncRNAs through sharing miRNAs. The ceRNA hypothesis elucidates the mechanism by which these RNAs compete to bind to miRNAs. Their disorders may lead to the occurrence and progression of cancer. Several studies have demonstrated that ceRNA is crucial in various cancers, including HCC [10,11]. Therefore, identifying and studying the role of ceRNAs in HCC development and progression is critical. The ceRNA disorder is closely related to multiple key processes in HCC cells, including enhanced proliferation, increased invasion and migration, enhanced metastatic potential, and the development of drug resistance. ceRNA disorder has been widely considered an important factor in the complex pathogenesis of HCC [12]. Many studies have revealed the profound impact of ceRNA disorder on multiple critical cellular processes, shaping the invasive phenotype of HCC cells. Aberrant ceRNA expression profiles are significantly associated with enhanced cell proliferation, promoting uncontrolled growth and expansion of HCC tumors. Moreover, disordered ceRNA networks are closely related to the enhanced invasion and migration of HCC cells, allowing them to infiltrate surrounding tissues and metastasize distally [13]. Furthermore, ceRNA disorder is strongly linked to the acquisition of drug resistance, presenting a significant challenge to the effective treatment of HCC. Overall, these findings underscore the complex interplay between ceRNA disorder and the malignant progression of HCC, highlighting the potential of ceRNA-based therapeutic strategies to combat this devastating disease.

However, current ceRNA research has some limitations. The interaction network between RNAs is complex, and current research makes it difficult to comprehensively and systematically reveal the overall framework and mechanism of the ceRNA network. In contrast, bioinformatic analysis has significant advantages in ceRNA research. It can utilize public databases to integrate multi-omics data from multiple samples and construct and explore ceRNA networks at a higher level. Bioinformatic methods can also discover potential rules of interaction between RNAs and provide a theoretical basis for further experimental verification. Bioinformatics prediction and screening can substantially reduce the amount of experimental work required and improve the research efficiency. It can effectively compensate for the limitations of experimental research and provide important references and a foundation for understanding the overall framework and deeper mechanisms of ceRNA regulatory networks. This study applied bioinformatics methods to analyze bulk and single-cell data to identify a new ceRNA network and explore the potential mechanisms regulating HCC progression.

The circHECTD1 is generated from its parental gene *HECTD1* through back-splicing. Studies have demonstrated that circHECTD1 is significantly upregulated in HCC [14] and gastric cancer [15] and can promote tumor progression through the ceRNA mechanism. In HCC, circHECTD1 facilitates the progression by targeting miR-485-5p to upregulate *MUC1*. In gastric cancer, circHECTD1 promotes tumor progression by targeting miR-1256 to activate the β-catenin/c-Myc signaling pathway. Nevertheless, the role of the large and complex ceRNA network in disease mechanisms cannot be thoroughly elucidated by a single regulatory axis; therefore, it is imperative to employ bioinformatics analysis to identify and screen multiple downstream targets and explore additional potential mechanisms.

In this study, we used bioinformatics methods to identify a new HCC-related ceRNA network from circHECTD1 and analyze the regulatory mechanisms of pivotal targets in the network from multiple perspectives. This network provides a valuable reference for studying the functions of ceRNA regulatory networks in HCC and proposes new targets and directions for diagnosing and treating HCC.

2. Materials and methods

2.1. Data download and preprocessing

We downloaded the sequence and related information for circHECTD1 (circ_0031450) from the circBASE database. We downloaded all circRNAs and their corresponding targets from the circBANK [16] (http://www.circbank.cn/searchCirc.html) database and used Strawberry Perl (https://strawberryperl.com/) to extract the circ_0031450 targets. We screened the miRNA array data from the Gene Expression Omnibus (GEO) [17] database (https://www.ncbi.nlm.nih.gov/geo/). The screening criteria were as follows: 1) The specimens used for sequencing were human liver tissues (normal and cancerous). 2) Both the normal and tumor group samples included more than six samples. 3) The datasets have either not been used or have been used infrequently by others besides the original authors. 4) The individuals from whom the sequencing samples were derived have not undergone pharmacological or other therapeutic interventions. Following the above criteria, we selected GSE39678, downloaded its expression matrix and platform file, and used R software (https://www.r-project.org/) and the limma package to analyze the dataset. Due to the sequencing depth issue with the miRNA data, we lowered the screening threshold. $|logFC| > 0.5$ and adjusted $P < 0.05$ were screening thresholds for the next analysis to obtain differentially expressed miRNAs. We downloaded transcriptome and clinical HCC data from The Cancer Genome Atlas (TCGA, https://portal.gdc.cancer.gov/) and used Perl to organize the data for gene expression and clinical information files. We then used R software and the limma package to perform differential gene expression analysis of the data. $|logFC| > 2$ and adjusted $P < 0.05$ were screening thresholds for the next analysis to achieve differentially expressed mRNAs in HCC. Simultaneously, we screened and downloaded recently released single-cell sequencing data of human HCC from the GEO database (GSE210679) for subsequent single-cell analysis. An ethical review was not required for this study.

2.2. Target prediction and ceRNA network construction

We selected the intersection of circ_0031450's target genes extracted from the circBANK database and differentially expressed miRNAs to identify the final circ_0031450 targets. These targets were used to predict their target mRNAs in the miRTarBase [18] (https://mirtarbase.cuhk.edu.cn/~miRTarBase/miRTarBase_2022/php/index.php) and Targetscan [19] (https://www.targetscan.

org/vert_72/) databases. Then, we used the intersection of the predicted targets from the aforementioned two databases and the differentially expressed mRNAs in HCC from the TCGA database to determine the miRNA targets. We then screened these targets to distinguish the unique targets of individual miRNAs or the common targets of multiple miRNAs to construct the ceRNA network. Based on the correspondence between circRNA-miRNA-mRNA, we created a network file and imported it into the Cytoscape [20] (https://cytoscape.org/) software to construct the ceRNA network. We used different colors, shapes, and connector lines to distinguish between different nodes or relationships between nodes.

2.3. Functional enrichment analysis of targets, PPI network construction, and key target screening

To clarify the main biological processes and signaling pathways enriched in the mRNAs of the ceRNA network, we conducted GO and KEGG enrichment analysis using R packages (clusterProfiler, org.Hs.eg.db, enrichplot, ggplot2, and ComplexHeatmap) and visualized the results. The adjusted *P*-value filter criterion was set at 0.05. The top 30 most significantly enriched biological processes or signaling pathways were displayed in bubble and circle charts. To elucidate the interaction between target proteins and screen out key targets, we imported the targets into the STRING [21] (https://cn.string-db.org/) database Multiple Protein module and selected "*Homo sapiens*" as the species. We then obtained a protein interaction network graph and hidden isolated nodes, and we selected the default parameters for the remaining. The results were imported into Cytoscape, and the STRINGify network function of the STRING plugin was used to visualize and beautify the network. We used the cytoHubba plugin to screen key nodes in the network. The parameters in the plugin were set as follows: 1) Node scoring method: calculation; 2) selecting the top 15 nodes with the highest scores; 3) algorithm: MCC; 4) display options: checking the first-stage nodes and displaying the expanded subnetwork. Finally, we exported the network graph and screened key target files.

2.4. Key target pathway activity and overall survival (OS) analysis

We clarified the key signaling pathways mainly activated or inhibited by key targets in HCC through the online analysis platform GSCALite [22] (http://bioinfo.life.hust.edu.cn/web/GSCALite/).We selected Pathway Activity as the analysis module. The results were then exported as heat maps and network graphs. Simultaneously, to clarify whether the expression of key targets was related to the survival prognosis of patients with HCC, we used the Kaplan-Meier Plotter [23] (https://kmplot.com/analysis/index.php?p=service) online analysis platform to perform an OS analysis on hub targets. We selected the mRNA RNA-seq expression dataset for HCC and exported the results after completing the analysis.

2.5. Immune and clinical correlation analysis

First, we used the limma package to extract the single-gene expression levels of key targets related to survival in the HCC transcriptome data, used the CIBERSORT [24] algorithm to calculate the correlation between each gene and immune cells, and visualized the results. The statistical method for the correlation test was "Spearman," and $P < 0.05$ was considered the screening threshold. We then screened out the targets related to immune infiltration for immune checkpoint analysis. We used the Gene Expression Profiling Interactive Analysis 2 [25] (GEPIA2, http://gepia2.cancer-pku.cn/#index) online analysis platform to analyze the correlation between the expression of targets and *PDCD1*, *CD274*, and *CTLA4*, three classic immune checkpoint molecules. The statistical method used for the correlation test was "Pearson," and $P < 0.05$ was considered the screening threshold. Finally, we screened out targets related to the survival, tumor-infiltrating immune cells, and immune checkpoints of patients with HCC as hub targets. Next, we performed a clinical correlation analysis of hub targets. We organized the clinical data of Liver hepatocellular carcinoma (LIHC) in the TCGA database and obtained clinical stage data for stages I, II, III, and IV by integrating substages into major stages. We then used R packages (limma, ggpubr) to analyze the correlation between the expression of hub targets and the clinicopathological stages of patients with HCC. The Wilcoxon test was used for statistical analysis, and $P < 0.05$ was considered the screening threshold.

2.6. Hub network construction, gene expression verification, and receiver operating characteristic (ROC) analysis

Following the relationship between elements, we extracted the corresponding miRNAs of the hub targets derived from the aforementioned analysis, generated a network file, and constructed a hub network using the Cytoscape software. We adjusted the parameters to ensure that the attributes and implications of each element in the hub network were consistent with those in the ceRNA network. According to the literature, circHECTD1 is highly expressed in HCC [14]. According to the ceRNA mechanism, its target miRNA expression should decrease, and the downstream mRNA expression should increase. Therefore, we verified the expression of circHECTD1 targets and downstream mRNAs in the dataset to clarify whether the constructed ceRNA network conforms to the ceRNA regulatory mechanism. We used R to evaluate the differential expression of miRNAs in the hub network between the normal and tumor groups in the GSE39678 dataset and visualized the results. We analyzed the differential expression of mRNAs in the hub network between the normal and tumor groups in TCGA-LIHC datasets and visualized the results. The Wilcoxon test was used for statistical analysis, and $P < 0.05$ was considered the screening threshold. Simultaneously, to determine whether the aforementioned targets have diagnostic value for HCC, we employed the pROC package to conduct ROC analysis on miRNAs and mRNAs in the hub network based on GSE39678 and TCGA-LIHC datasets, respectively. An area under the curve (AUC) > 0.7 was considered to indicate the diagnostic value of the target for HCC.

2.7. Related gene prediction and functional enrichment analysis of hub genes

We predicted genes related to hub targets and performed GO and KEGG enrichment analyses to verify whether the targets obtained through the above analysis steps have major molecular functions in the PPI and ceRNA networks. We used a similar gene detection module of the GEPIA2 analysis platform to predict the top 150 genes related to hub targets. We then performed enrichment analysis using the same analysis methods and the R packages as before. The adjusted P-value filter criterion was set at 0.05. The top 30 most significantly enriched GO and KEGG pathways were identified. We compared the final enrichment results with those obtained in Steps 1.3 and 1.4 for confirmatory validation.

2.8. Verification of hub gene expression in single-cell data

The conditions for initial data filtering were as follows: 1) At least one gene was detected in at least three cells, and 2) the minimum number of genes detected in each cell was 200. The data filtering conditions were as follows: retaining cells with 200–8000 detected genes and a mitochondrial percentage of less than 5 %. The data were normalized using the NormalizeData function. We implemented principal component analysis to reduce the dimensionality of the data and presented the top 20 Principal Components (PCs) in a heat map. Combined with the JackStraw and ElbowPlot functions, we selected 16 PCs for the subsequent analysis. We selected the optimal resolution as 1.5 to cluster cells based on FindNeighbors and clustree functions. We used the nonlinear dimensionality reduction method Uniform Manifold Approximation and Projection (UMAP) to visualize the cell cluster results and used the FindAllMarkers function to identify marker genes for each cluster. We annotated the cell subpopulations using the SingleR package, checked the annotation results based on the marker genes of each annotated subpopulation, and performed manual annotation of the annotation results as needed based on the CellMarker website (http://xteam.xbio.top/CellMarker/). Finally, we visualized the expression of the hub genes in each cell subpopulation.

3. Results

3.1. Data and target preprocessing

A total of 138 circ_0031450 targets were extracted from the target data in the circBANK database. Ninety-two differentially expressed miRNAs were analyzed using the chip dataset. By considering the intersection, four final circ_0031450 targets were obtained (Fig. 1A), namely miR-548c-5p, miR-548d-5p, miR-648, and miR-764. Using TCGA-LIHC, 3457 differentially expressed mRNAs were identified. In total, 598 targets were predicted using the miRTarBase database. A total of 9311 targets were predicted using the TargetScan database. By taking the intersection of the above differentially expressed mRNAs, miRTarBase, and TargetScan databases, 102 targets of miRNAs were obtained (Fig. 1B). We screened and sorted the four miRNAs and 102 mRNAs to match the unique or common targets of individual or multiple miRNAs for subsequent analysis. The final targets were sorted as follows: *ANP32B*, *AQP3*, *CBX3*, DDB1, EBNA1BP2, ERH, ESYT1, GIMAP4, GTPBP2, HSP90AA1, KHSRP, KIF2C, *MAP2K1*, *PRELID1*, *PTBP1*, *SPCS3*, *SPRYD4*, *UBE2D2*, *VDAC2* and *XRCC6* as common targets of miR-548c-5p and miR-548d-5p; *ACP1*, *ARL5B*, *CAPZA1*, *CSE1L*, *MAP2K4*, *PCGF5*, *RAB1A* and *TNIP2* as the common targets of miR-548c-5p, miR-548d-5p, and miR-648; *ACSM2B*, *ACTN4*, *ANGPTL3*, *C1orf43*, *CCNB1*, *CDK4*, *CNBP*, *COLGALT1*, *DHTKD1*, *FCN2*, *GNPNAT1*, *HMGN2*, *MCC*, *MELK*, *MFSD2A*, *MKI67*, *MPZL1*, *NSMCE2*, *PPARA*, *PPP1R15B*,
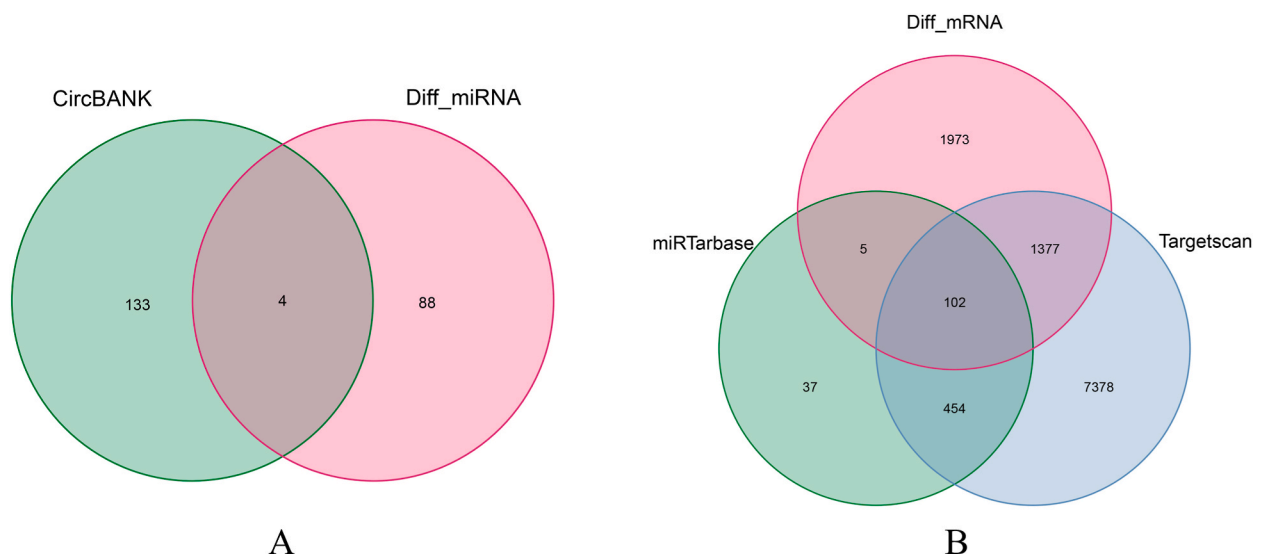

Fig. 1. Target prediction results. (**A**) Targets of circ_0031450. (**B**) Targets of miR-548c/d-5p, miR-764, and miR-648.
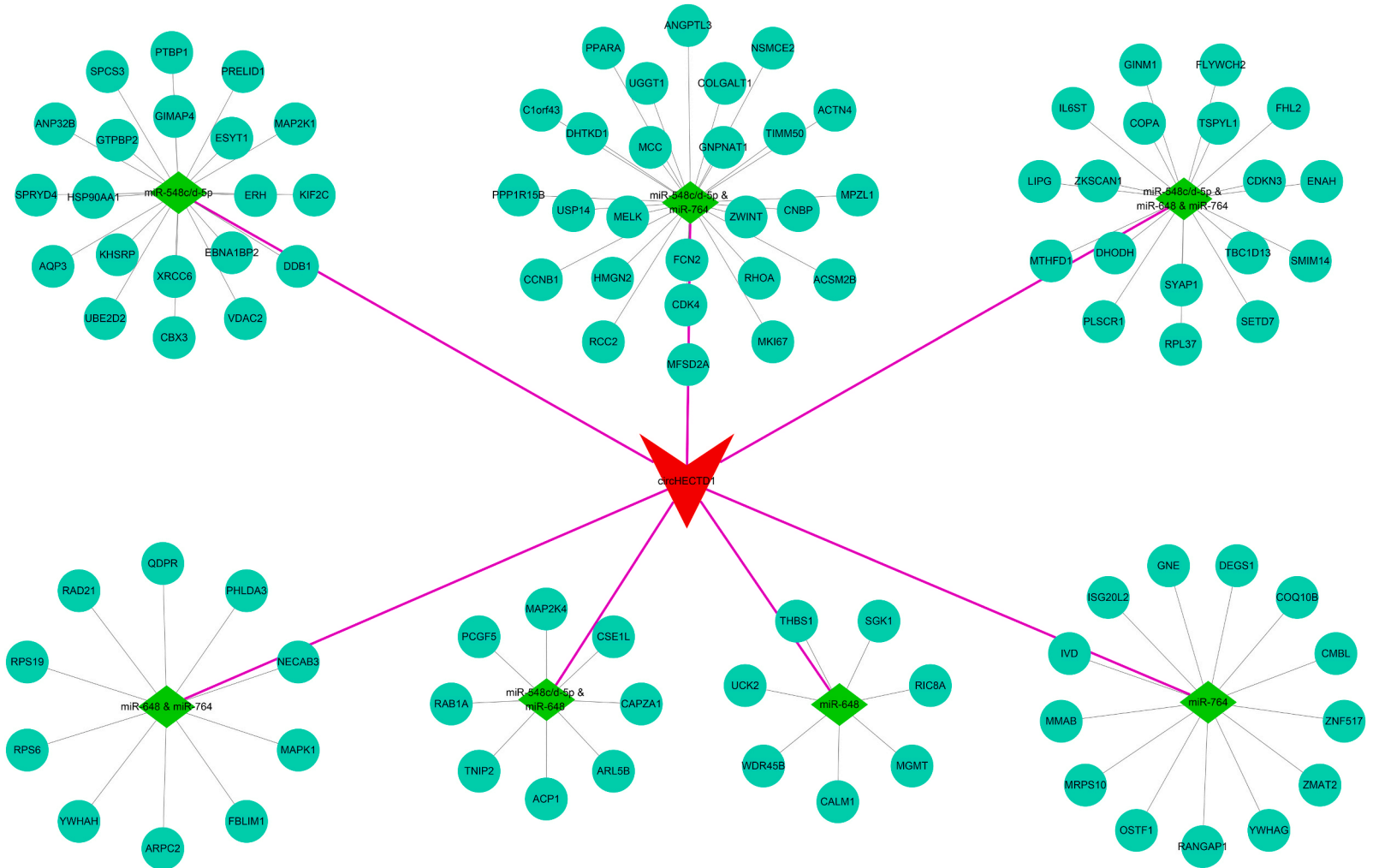
Fig. 2. ceRNA network. In the diagram, the central V-shaped red element represents circHECTD1, green diamond-shaped elements represent miRNAs, and circular elements represent mRNAs.

RCC2, *RHOA*, *TIMM50*, *UGGT1*, *USP14* and *ZWINT* as the common targets of miR-548c-5p, miR-548d-5p, and miR-764; *CALM1*, *MGMT*, *RIC8A*, *SGK1*, *THBS1*, *UCK2* and *WDR45B* as the targets of miR-648; *ARPC2*, *FBLIM1*, *MAPK1*, *NECAB3*, *PHLDA3*, *QDPR*, *RAD21*, *RPS19*, *RPS6* and *YWHAH* as the targets of miR-648 and miR-764; *CMBL*, *COQ10B*, *DEGS1*, *GNE*, *ISG20L2*, *IVD*, *MMAB*, *MRPS10*, *OSTF1*, *RANGAP1*, *YWHAG*, *ZMAT2* and *ZNF517* as the targets of miR-764; *CDKN3*, *COPA*, *DHODH*, *ENAH*, *FHL2*, *FLYWCH2*, *GINM1*, *IL6ST*, *LIPG*, *MTHFD1*, *PLSCR1*, *RPL37*, *SETD7*, *SMIM14*, *SYAP1*, *TBC1D13*, *TSPYL1* and *ZKSCAN1* as the common targets of miR-548c-5p, miR-548d-5p, miR-648 and miR-764.

3.2. Construction of the ceRNA network

The Cytoscape software successfully constructed a ceRNA network containing 110 nodes and 109 connection edges (Fig. 2). The red V-shaped element in the figure represents circHECTD1. Green diamond elements represent miRNAs. Blue circular elements represent mRNAs. The thick purple lines represent the target relationships between the circRNAs and miRNAs. Thin gray lines represent the target relationships between miRNAs and mRNAs.
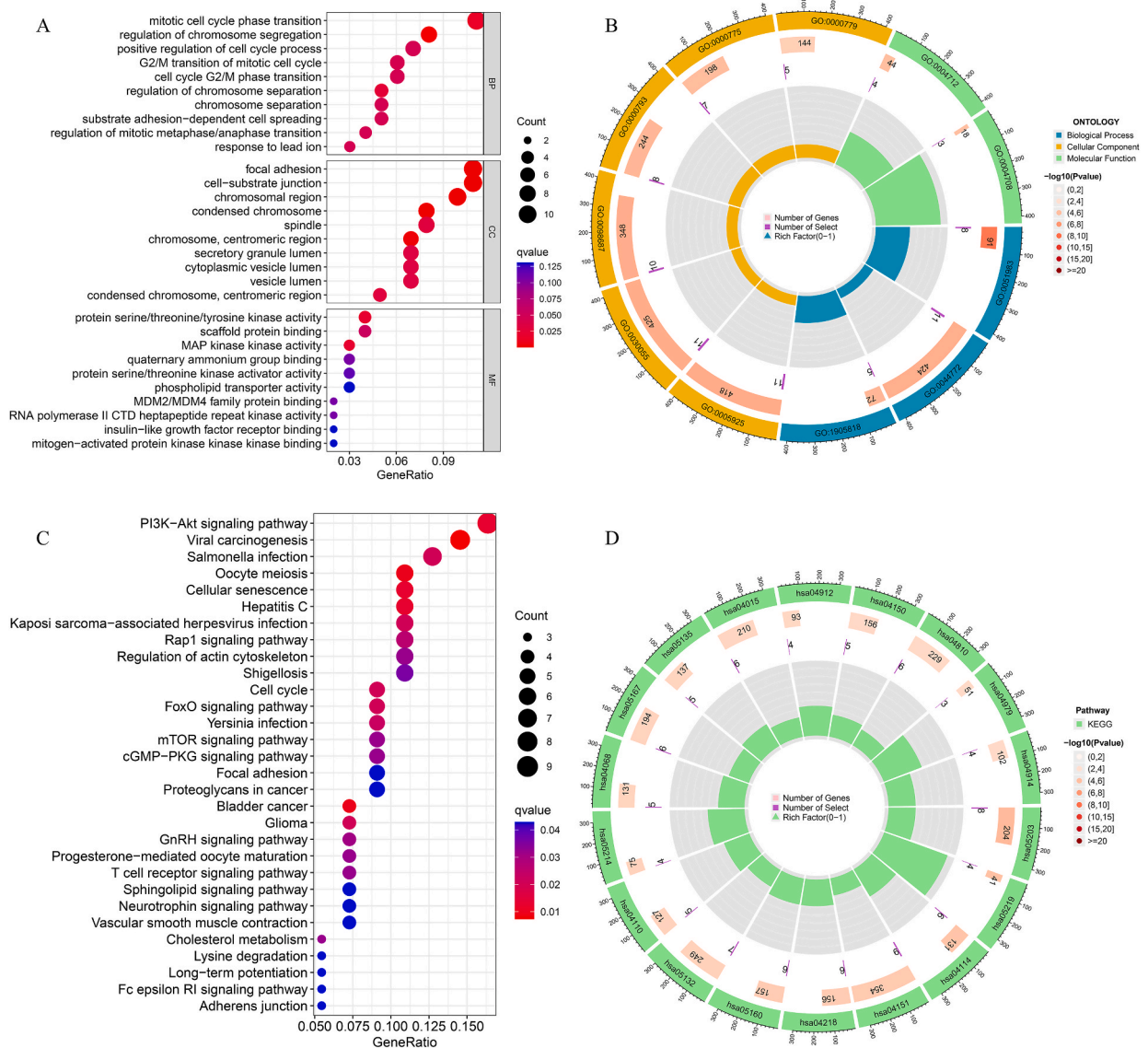

Fig. 3. GO and pathway enrichment analyses. (**A-B**) Bubble and circle diagrams of GO enrichment. (**C-D**) Bubble and circle diagrams of KEGG enrichment.

3.3. GO and KEGG enrichment analysis

The GO enrichment analysis of the targets yielded 34 entries (Fig. 3A and B). The main enriched biological processes (BP) were mitotic cell cycle phase transition (GO: 0044772) and regulation of chromosome segregation (GO: 0051983). The main enriched cell components (CC) were focal adhesion (GO: 0005925), cell-substrate junction (GO: 0030055), chromosomal region (GO: 0098687), and condensed chromosomes (GO: 0000793). The main enriched molecular functions (MF) were protein serine/threonine/tyrosine kinase activity (GO: 0004712) and mitogen-activated protein (MAP) kinase activity (GO: 0004708). Fig. 3A depicts a bubble chart of GO enrichment analysis. The horizontal coordinates represent the proportion of genes enriched in the corresponding entries. The vertical coordinates represent the enriched GO entries. The larger the bubble diameter, the more significant the enrichment. The redder the bubble color, the smaller the *q* value. Fig. 3B displays a circular chart of the GO enrichment. The outermost circle represents the ID number of GO entries. Blue, yellow, and green represent the BP, CC, and MF, respectively. The second circle represents the significance of enrichment; the redder the color, the more significant the enrichment. The innermost circle represents the size of the enrichment factor. KEGG pathway enrichment analysis of the targets yielded 51 signaling pathways (Fig. 3C and D). The significantly enriched pathways included the phosphatidylinositol 3-kinase-protein kinase B (PI3K-Akt) signaling pathway (hsa04151), viral carcinogenesis (hsa05203), cellular senescence (hsa04218), hepatitis C (hsa05160), and cell cycle (hsa04110). Fig. 3C illustrates a bubble chart of KEGG enrichment analysis. The horizontal coordinates represent the proportion of genes enriched in the corresponding pathways. Vertical coordinates represent enriched pathways. The larger the bubble diameter, the higher the proportion of genes enriched in the corresponding pathway. The redder the bubble color, the more significant the enrichment. Fig. 3D depicts a circular chart of the KEGG enrichment. The outermost circle represents the ID number of the pathway. The second circle represents the significance and proportion of the genes enriched in the corresponding pathways. The redder the color, the more significant the enrichment.

3.4. Constructing PPI network and screening key targets

We successfully constructed a PPI network comprising 68 nodes and 150 edges (Fig. 4A). Nodes of different colors represent different proteins, and the strip structure in the center of the protein shows the simulated three-dimensional structure of the protein. Gray lines represent the interactions between proteins. Using the CytoHubba plugin, we obtained a network containing 15 key targets and 49 edges. Through network expansion, an expanded network containing 45 nodes and 120 edges was obtained (Fig. 4B). The red and yellow nodes in the figure represent key targets: *YWHAG, YWHAH, MAP2K1, CCNB1, PPARA, ZWINT, CDK4, RHOA, MELK, HSP90AA1, CDKN3, KIF2C, MKI67, MAPK1,* and *RPS6.* Nodes with a darker red color indicate that the node rank is higher. The blue nodes are other nodes in the PPI network that interact with key targets.

3.5. Pathway activity analysis and survival analysis

Pathway activity analysis of key targets suggested that their expression of key targets mainly activates the cell cycle and apoptosis
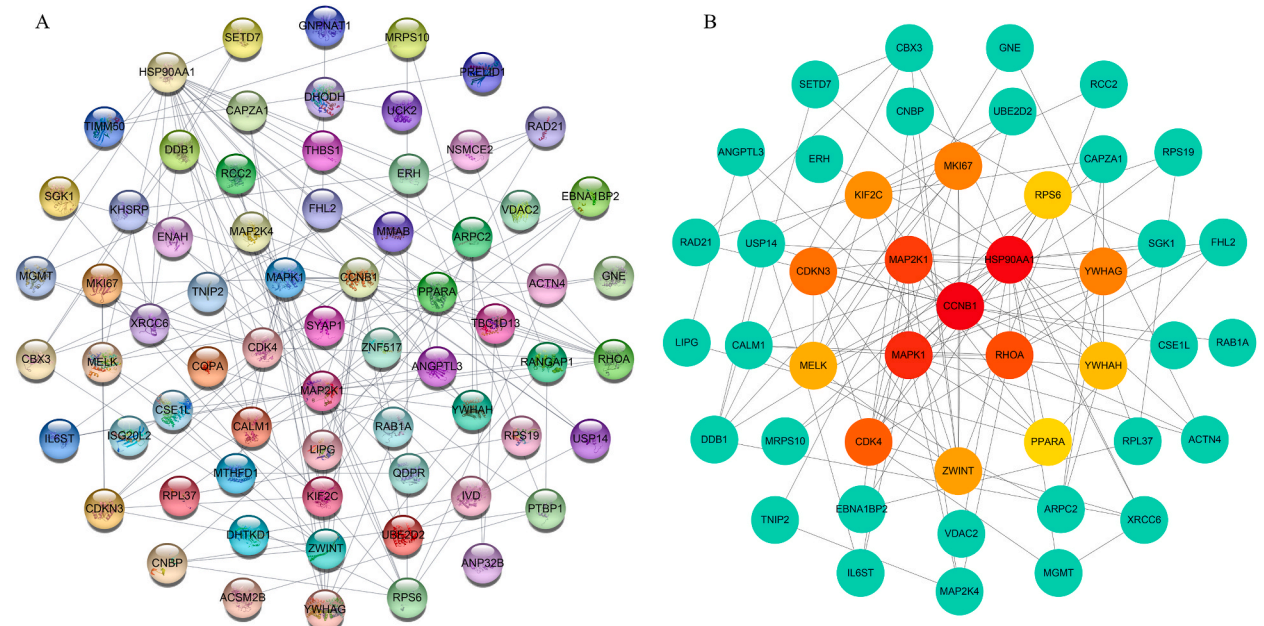

Fig. 4. PPI network and the key targets screening. (**A**) The PPI network. (**B**) Key targets screened using the CytoHubba plugin.

Fig. 5. Pathway activity, survival, and immune cell infiltration analyses. (**A-B**) Heatmap and network of pathway activity analysis. (**C**) OS analysis. (**D**) Spearman's correlation analysis of survival-related targets and immune cell expression. SCC: Spearman correlation coefficient.

pathways and inhibits the hormone estrogen receptor (ER) and rat sarcoma/mitogen-activated protein kinase (RAS/MAPK) pathways (Fig. 5A). It is noteworthy that *ZWINT, MKI67, MELK, KIF2C, CDKN3,* and *CCNB1* exhibited activating effects in more than 60 % of tumors on the cell cycle pathway, the most significant of which were *KIF2C* (75 %) and *CCNB1* (75 %). In LIHC, the main effects of key targets on pathway activity were to activate cell cycle, apoptosis, and EMT pathways and inhibit the hormone estrogen receptor/ androgen receptor (ER/AR), RAS/MAPK and receptor tyrosine kinase (RTK) pathways (Fig. 5B). Fig. 5A presents a heatmap of the
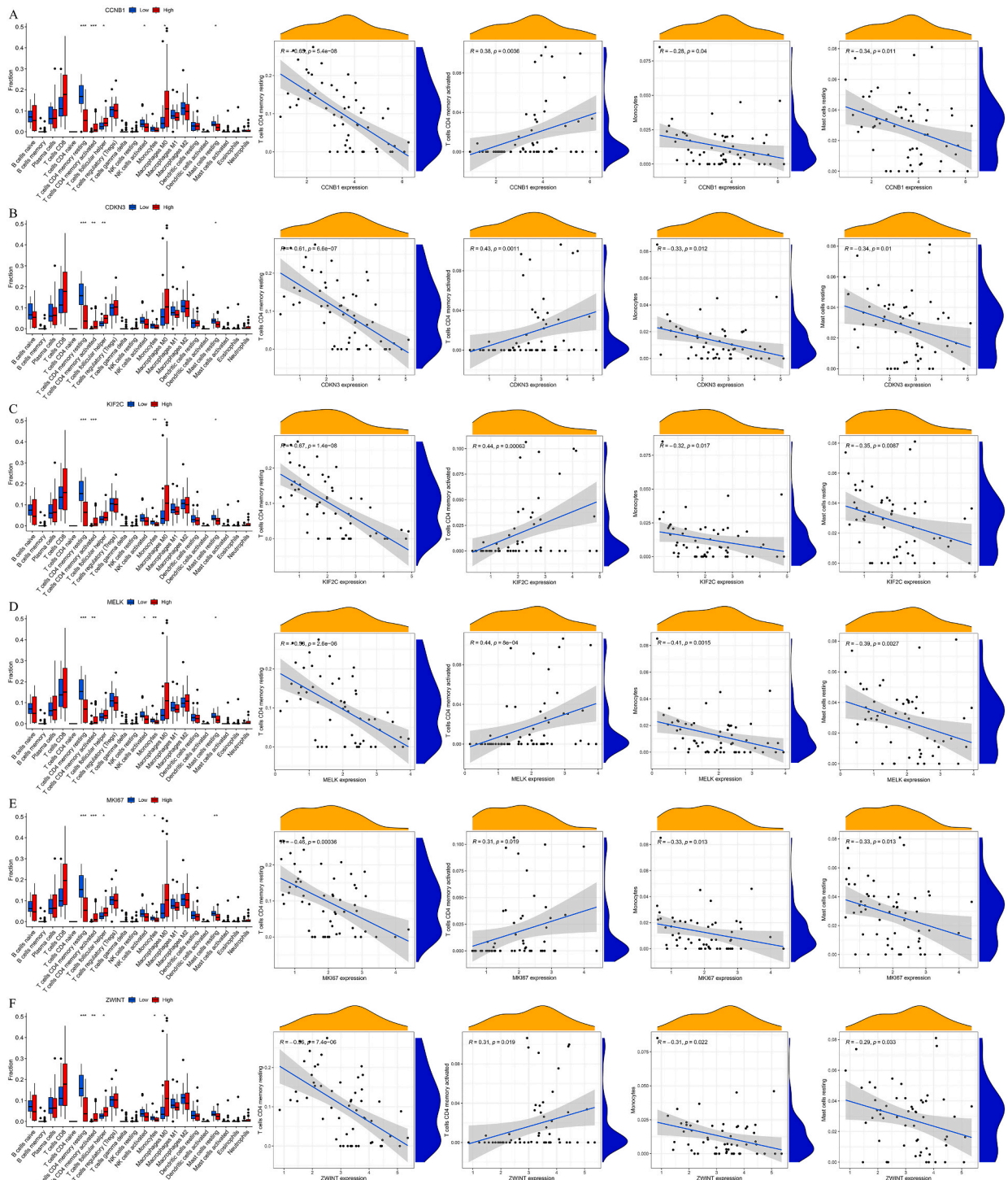

Fig. 6. Targets that have a good correlation with immune cells. (**A–F**) *CCNB1, CDKN3, KIF2C, MELK, MKI67,* and *ZWINT,* respectively.

pathway activity analysis. The horizontal axis is ten classic signaling pathways associated with tumors, and the vertical axis is a key target. The values in the heatmap represent the percentage of gene expression that can activate or inhibit the corresponding pathway in 33 types of tumors. Positive red values in the heatmap indicate activation, negative blue values indicate inhibition, and darker colors
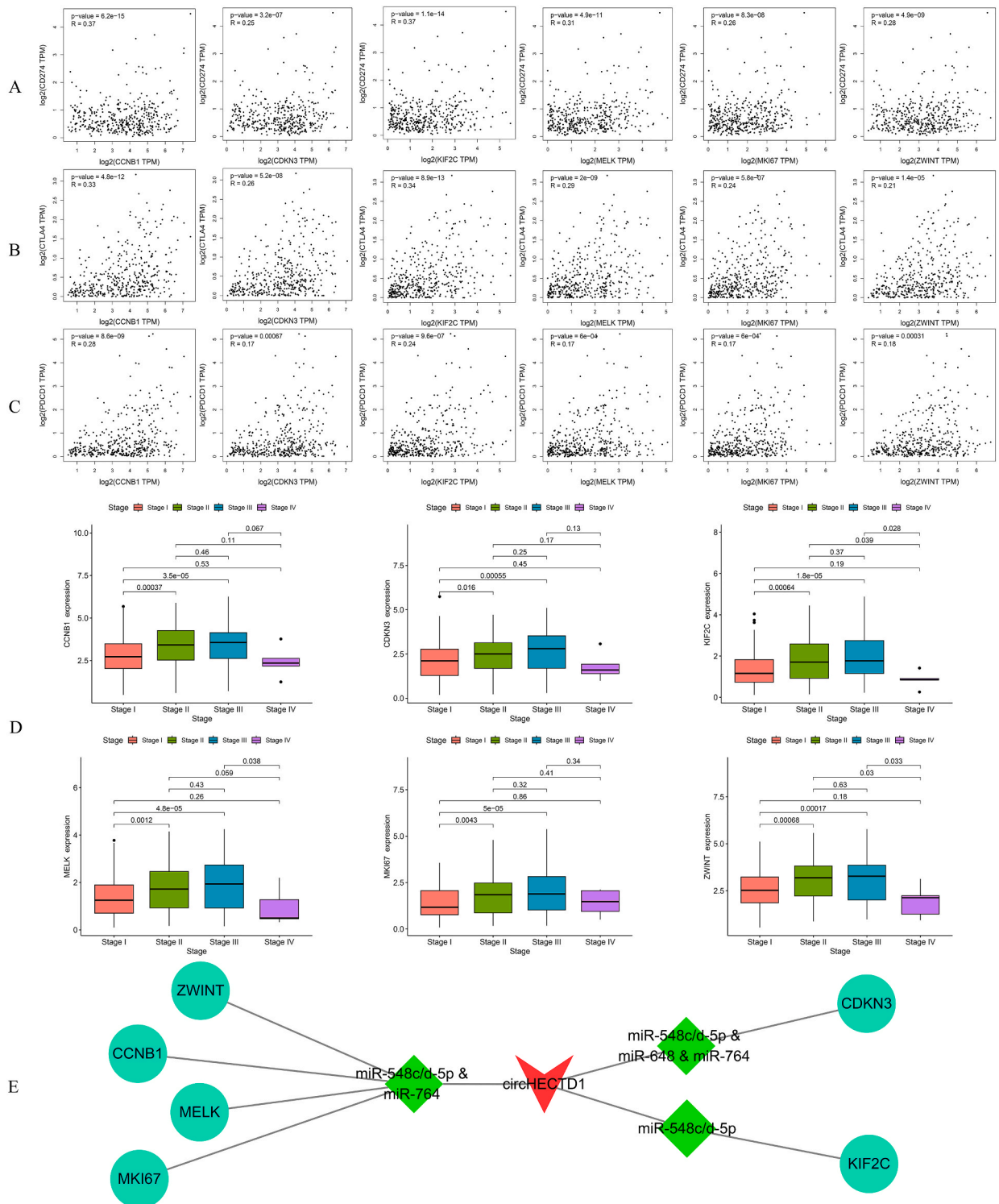

Fig. 7. Immune checkpoint analysis, clinical stage correlation analysis, and hub network construction. (A–C) Correlation analysis between hub targets and *CD274*, *CTLA4*, and *PDCD1*. (D) Correlation between hub target expression and clinical stage of patients with HCC. (E) The hub network.

indicate a higher percentage. Fig. 5B illustrates a network diagram of the relationship between key targets and pathway activity in LIHC. Solid lines indicate activation, and dashed lines indicate inhibition. Simultaneously, to clarify the relationship between key targets and the prognosis of patients with HCC, we conducted an OS analysis. The results revealed that *CCNB1* ($P = 3.4e-05$), *CDK4* ($P = 3e-05$), *CDKN3* ($P = 0.0066$), *HSP90AA1* ($P = 0.0028$), *KIF2C* ($P = 1.7e-06$), *MAP2K1* ($P = 0.048$), *MELK* ($P = 3.7e-05$), *MKI67* ($P = 0.00011$), *PPARA* ($P = 0.013$), *RHOA* ($P = 0.016$), *YWHAH* ($P = 0.0025$), and *ZWINT* ($P = 8.5e-07$) were associated with the prognosis
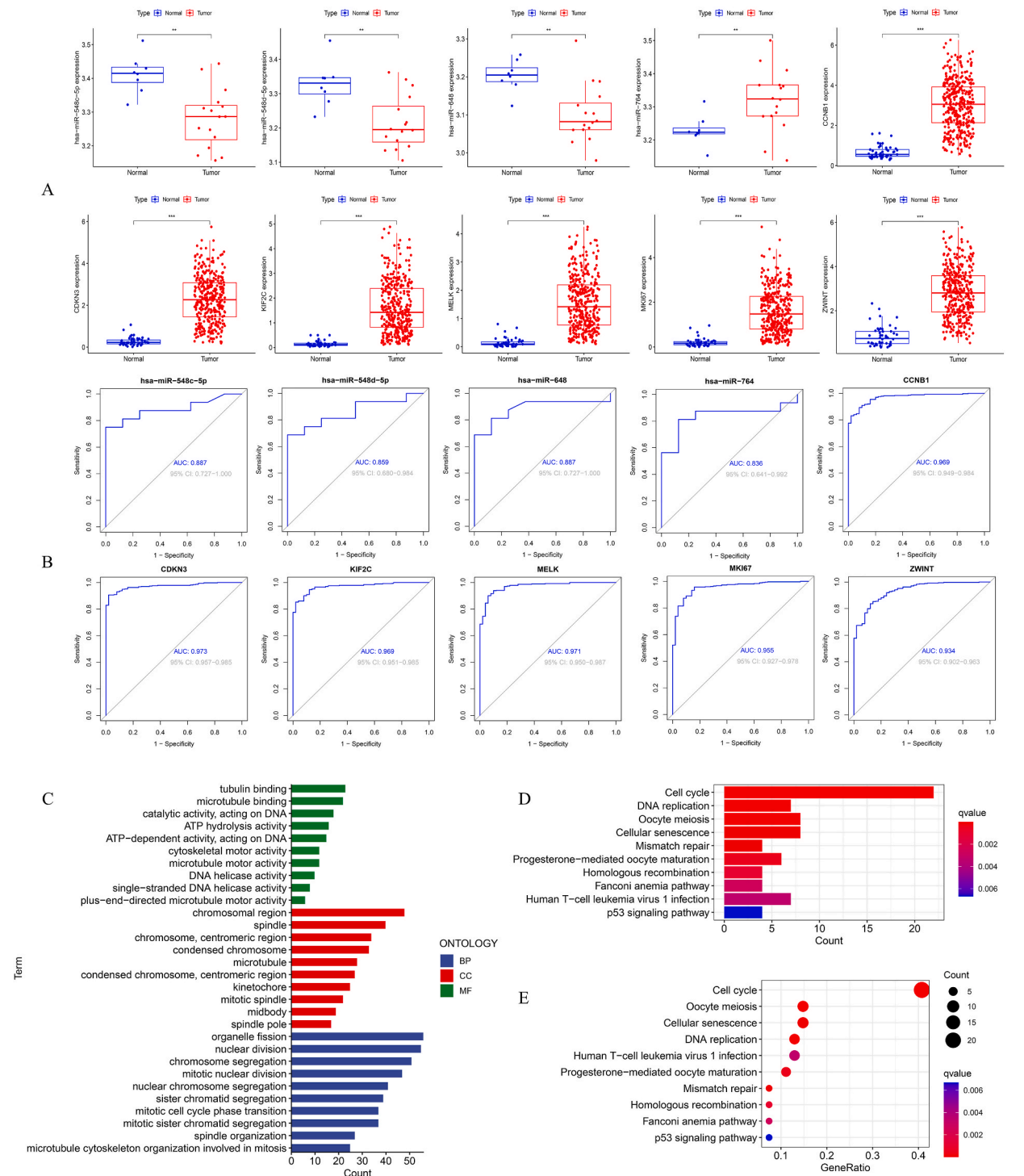

Fig. 8. Expression analysis, gene prediction, and functional analysis. (**A-B**) Expression and ROC analysis of all targets. (**C**) GO enrichment analysis of predicted genes. (**D-E**) KEGG enrichment analysis.
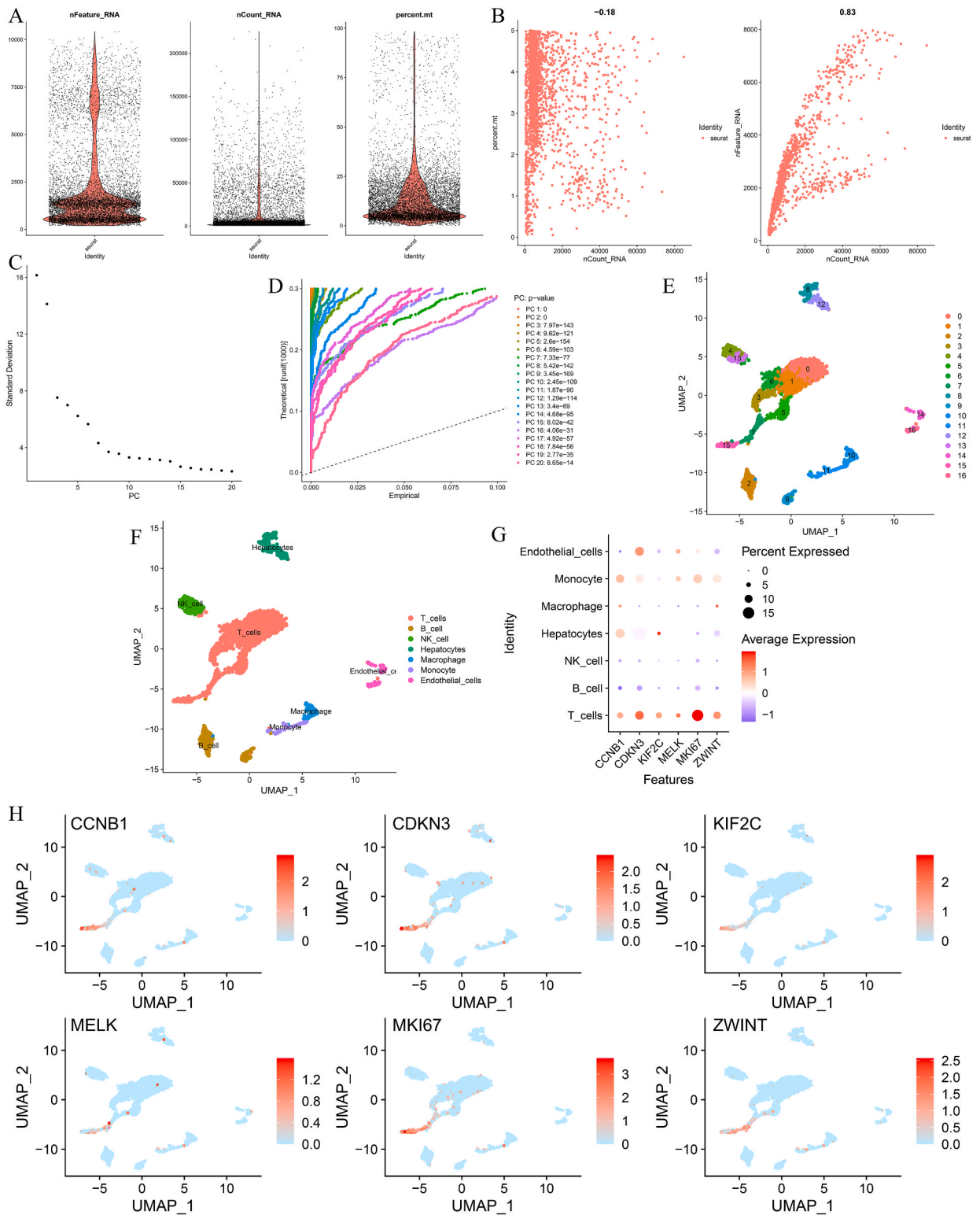
Fig. 9. Sing-cell analysis. (**A-B**) The features of single-cell data. (**C-D**) Elbow and JackStraw diagrams of 20 PCs. (**E-F**) Cell clustering and subpopulation annotation diagrams. (**G**) Bubble map of the relative expression of hub targets in the cell subsets. (**H**) Scatter plots of CCNB1, CDKN3, KIF2C, MELK, MKI67, and ZWINT expression.

of patients with HCC (Fig. 5C). The prognosis of patients with HCC was better in the low expression groups of *CCNB1*, *CDK4*, *CDKN3*, *HSP90AA1*, *KIF2C*, *MELK*, *MKI67*, *RHOA*, *YWHAH*, and *ZWINT*, whereas the prognosis was worse in the low expression groups of *MAP2K1* and *PPARA*.

3.6. Immune and clinical correlation analysis

The results revealed that these survival-related targets were correlated with the expression levels of immune cells (Fig. 5D). The expressions of *CCNB1* (Fig. 6A), *CDKN3* (Fig. 6B), *KIF2C* (Fig. 6C), *MELK* (Fig. 6D), *MKI67* (Fig. 6E), and ZWINT (Fig. 6F) were well correlated with immune cell contents in the tumor immune microenvironment of HCC, and the results were consistent. We demonstrated that the expression of the above targets was positively correlated with the content of T cells CD4 memory activated in the tumor immune microenvironment of HCC and negatively correlated with T cells CD4 memory resting monocytes and resting mast cells. Immune checkpoint analysis indicated that hub target expression was positively correlated with expressions of CD274 (Fig. 7A), *CTLA4* (Fig. 7B), and *PDCD1* (Fig. 7C). Clinical correlation analysis suggested that the hub targets were associated with the clinical staging of patients with HCC (Fig. 7D).

3.7. Gene expression and ROC analysis

Based on the relationship between nodes in the ceRNA network, we extracted the common hub targets of miR-548c/d-5p as KIF2C; the common targets of miR-548c/d-5p and miR-764 were *CCNB1*, *MELK*, *MKI67*, and *ZWINT*; the common targets of miR-548c/d-5p, miR-648 and miR-764 were *CDKN3*. Accordingly, a hub network was created (Fig. 7E). The results of gene expression analysis in the dataset showed that miR-548c-5p, miR-548d-5p, and miR-648 were expressed at low levels in the HCC tumor group, whereas miR-764 was highly expressed in the tumor group. *CCNB1*, *CDKN3*, *KIF2C*, *MELK*, *MKI67,* and *ZWINT* were highly expressed in the HCC tumor group (Fig. 8A). ROC analysis revealed that the AUC of the above targets for diagnosing HCC was >0.7, indicating that they had good diagnostic value for HCC (Fig. 8B).

3.8. Prediction and functional enrichment analysis of hub target-related genes

In total, 150 hub target-related genes were identified. Pearson's correlation coefficient between these genes and hub targets was greater than or equal to 0.78, indicating that the prediction results were highly credible. GO enrichment analysis of these genes suggested 420 enriched GO entries. The most significantly enriched BPs were nuclear division (GO: 0000280), chromosome segregation (GO: 0007059), and mitotic cell cycle phase transition (GO: 0044772). The most significantly enriched CCs were chromosomal region (GO: 0098687) and condensed chromosome (GO: 0000793). The most significantly enriched MFs were microtubule binding (GO: 0008017), ATP-dependent activity acting on DNA (GO: 0008094), and tubulin binding (GO: 0015631) (Fig. 8C). KEGG enrichment analysis enriched 10 signaling pathways with statistical significance, including cell cycle (hsa04110), DNA replication (hsa03030), oocyte meiosis (hsa04114), cellular senescence (hsa04218), mismatch repair (hsa03430) and p53 signaling pathway (hsa04115; Fig. 8D and E).

3.9. Validation of hub gene expression in single-cell datasets

The dataset contained 9,439 cells and detected 21783 genes. The basic characteristics of the data are displayed in Fig. 9A. After data filtering, 2,584 cells were included in the subsequent analysis. A correlation analysis between the characteristics (Fig. 9B) confirmed the good data quality. After data dimensionality reduction, according to ElbowPlot (Fig. 9C) and JackStraw (Fig. 9D) graphs, the first 16 PCs and the best resolution of 1.5 were selected for subsequent analysis, and 17 cell clusters were obtained (Fig. 9E). Cell subpopulation annotation revealed seven cell types, including T, B, and NK cells (Fig. 9F). Simultaneously, the analysis indicated that hub genes were highly expressed in T and mononuclear cells (Fig. 9G and H).

4. Discussion

In this study, we constructed a ceRNA network mediated by circHECTD1 and identified its important hub targets using bioinformatics analysis. These hub targets are mainly involved in regulating the cell cycle, apoptosis, and EMT pathways and affect the tumor immune microenvironment of HCC, thereby further affecting the prognosis of patients with HCC. Studies have revealed that circHECTD1 is highly expressed in HCC and may promote tumor progression [14]. However, according to the ceRNA mechanism, its target miRNAs should be expressed at low levels, while downstream mRNAs should be highly expressed. This study found that, except for miR-764, the three target miRNAs of circHECTD1, namely miR-548c-5p, miR-548d-5p, and miR-648, were lowly expressed in HCC, whereas their downstream hub targets *KIF2C*, *CCNB1*, *CDKN3*, *MELK*, *MKI67*, and *ZWINT* were highly expressed in HCC, which is consistent with the ceRNA mechanism, indicating that the constructed ceRNA network exhibited certain accuracy and credibility. In summary, the bioinformatics analysis in this study revealed that at a higher level, the ceRNA mechanism mediated by circHECTD1 may play a regulatory role in the occurrence and development of HCC.

We successfully screened 15 key targets in the ceRNA network. These targets mainly regulate the HCC progression by activating signaling pathways, including the cell cycle and apoptosis, and inhibiting signaling pathways, including hormone receptors and RAS/ MAPK. This result is consistent with the biological functions closely related to the occurrence and development of HCC reported in the

literature [26–28]. The cell cycle refers to a series of complex molecular events and regulatory mechanisms involved in its life cycle. The normal cell cycle regulates the cell from initiation to apoptosis in an orderly manner. When this process becomes disordered, the cell cycle may become out of control, and the occurrence of tumors becomes possible [29]. Abnormal regulation of the cell cycle pathway in HCC may be an important mechanism in the occurrence and development of HCC. An in-depth study of the abnormal regulation of the cell cycle pathway is of great significance for understanding the HCC mechanism and developing new treatment strategies. Studies have demonstrated that circBACH1 can inhibit p27 translation, thereby affecting the cell cycle process and ultimately promoting the progression of HCC as an oncogene [30]. Apoptosis is an important form of cell death that plays a key role in maintaining the balance of cell numbers in the body, eliminating abnormal cells, and inhibiting tumor development. The apoptosis signaling pathway involves a series of molecular signal transduction mechanisms that regulate apoptosis. Abnormal regulation of the apoptotic signaling pathway in HCC is closely related to the occurrence, development, and treatment resistance of tumors. The ceRNA mechanism affects HCC progression by regulating apoptosis [28,31]. In HCC, the occurrence and regulation of EMT are closely related to tumor invasion, metastasis, and treatment resistance. Multiple signaling pathways are involved in the EMT process of HCC cells, including Wnt/β-catenin, transforming growth factor-beta (TGF-β), Notch and Hedgehog [12,32,33]. Survival analysis results indicated that the expression of 12 key targets, including *CCNB1, CDK4, CDKN3, MELK,* and *MKI67,* is significantly associated with the survival prognosis of patients with HCC. These targets may affect patient prognosis by regulating HCC cell proliferation.

Further analysis revealed that six targets (*CCNB1, CDKN3, KIF2C, MELK, MKI67,* and *ZWINT*) were associated with immune infiltration and immune checkpoint expression in patients with HCC, suggesting that these six targets may not only directly regulate tumor cell growth but also participate in developing HCC by regulating the tumor immune microenvironment. This result is consistent with reports that *CCNB1* [34], *CDKN3* [35], *KIF2C* [36], and *MKI67* [37] have been confirmed to play an important role in immune receptors and related cells in patients with HCC. Therefore, these six targets may affect the prognosis of patients with HCC through immune-related mechanisms, providing a theoretical basis for treating HCC. Studies on the tumor microenvironment have recently become a hot topic in tumor research. Research on the immune microenvironment provides novel insights into tumor treatment [38, 39]. The ceRNA mechanism can regulate the tumor and immune microenvironments of HCC, thereby affecting disease development and guiding targeted treatment of HCC [40–42].

We observed that circHECTD1 directly regulates downstream targets, including CCNB1, MELK, MKI67, and *ZWINT,* by regulating miR-548c/d-5p and miR-764 and also indirectly affects the immune microenvironment and prognosis of patients with HCC by regulating immune-related targets, including *CDKN3* and *KIF2C*. This suggests that the constructed ceRNA network may play a role through multiple mechanisms. We incorporated these immune-related key targets and their corresponding miRNAs into the hub network and verified them through functional enrichment and gene expression analysis. The results showed that the functional enrichment of related genes was relatively consistent with our previous ceRNA network's results, further confirming the constructed hub network's reliability. Simultaneously, single-cell data analysis identified that hub genes were relatively highly expressed in T-cells and mononuclear cells of patients with HCC, consistent with our results of immune correlation analysis. This indicates that the ceRNA and hub networks regulated by circHECTD1 may affect the immune status and prognosis of patients with HCC by regulating T-cells and tumor-associated macrophages. Simultaneously, six hub targets were correlated with the clinical staging of patients with HCC and performed well as HCC diagnostic markers.

Although our study provides new insights into the potential role of the ceRNA and hub networks regulated by circHECTD1 in HCC development, some limitations still exist. First, our research was mainly based on bioinformatics analysis, and further mechanistic verification is required. For instance, in the ceRNA network we constructed, the miR-764 expression level did not align with our expectations, and further validation is required to determine whether the expression levels of other downstream mRNA targets thoroughly meet our expectations. Although the model is imperfect, we believe that it remains accurate and provides valuable insights into the role of ceRNA networks in diseases. The accuracy of our model does not rely entirely on the performance of a single miRNA but on the comprehensive behavior of the entire network. Moreover, ncRNA and its interaction networks are abnormally complex. We only focused on the regulatory network of circHECTD1; other ncRNAs and related networks may also play an important role in HCC, requiring further study. Moreover, the occurrence and development of HCC involve the interaction and imbalance of multiple biological processes and signaling pathways. Our research mainly focused on immune- and cell-cycle-related mechanisms; other mechanisms, including angiogenesis, apoptosis, and metastasis, are also important for future research.

In summary, our study preliminarily explored the potential role of ceRNAs and hub networks regulated by circHECTD1 in HCC development. This study suggests that this network may promote the occurrence and development of HCC by affecting the cell cycle, apoptosis, and the tumor immune microenvironment. Our research offers new insights into the role of ncRNA regulatory networks in HCC and treatment strategies for HCC. Future research can further confirm and explore this network's role and potential therapeutic targets in the occurrence and development of HCC.

Funding

Ethics declarations

This study does not require ethical review.

Data availability statement

All data used in this work could obtained from the mentioned online websites or databases in the paper. In addition, the accession number for the miRNA array dataset is GSE39678, and the accession number for the liver cancer single-cell dataset is GSE210679.

CRediT authorship contribution statement

Shuiqing Lan: Writing – original draft. **Guoqiang Zhong:** Writing – review & editing, Visualization, Validation, Supervision, Software, Resources, Project administration, Methodology, Investigation, Formal analysis, Data curation, Conceptualization.

Declaration of competing interest

The authors declare that they have no known competing financial interests or personal relationships that could have appeared to influence the work reported in this paper.

Acknowledgments

None.

References

[1] H. Rumgay, M. Arnold, J. Ferlay, O. Lesi, C.J. Cabasag, J. Vignat, M. Laversanne, K.A. McGlynn, I. Soerjomataram, Global burden of primary liver cancer in 2020 and predictions to 2040, J. Hepatol. 77 (2022) 1598–1606, https://doi.org/10.1016/j.jhep.2022.08.021.

[2] R.S. Finn, A.X. Zhu, Evolution of systemic therapy for hepatocellular carcinoma, Hepatology (Baltimore, Md (73 Suppl 1) (2021) 150–157, https://doi.org/10.1002/hep.31306.

[3] A. Villanueva, Hepatocellular carcinoma, N. Engl. J. Med. 380 (2019) 1450–1462, https://doi.org/10.1056/NEJMra1713263.

[4] J.M. Llovet, R. Pinyol, R.K. Kelley, A. El-Khoueiry, H.L. Reeves, X.W. Wang, G.J. Gores, A. Villanueva, Molecular pathogenesis and systemic therapies for hepatocellular carcinoma, Nat Cancer 3 (2022) 386–401, https://doi.org/10.1038/s43018-022-00357-2.

[5] H.L. Sanger, G. Klotz, D. Riesner, H.J. Gross, A.K. Kleinschmidt, Viroids are single-stranded covalently closed circular RNA molecules existing as highly base-paired rod-like structures, Proc. Natl. Acad. Sci. U.S.A. 73 (1976) 3852–3856, https://doi.org/10.1073/pnas.73.11.3852.

[6] Y. Seo, J. Rhim, J.H. Kim, RNA-binding proteins and exoribonucleases modulating miRNA in cancer: the enemy within, Exp. Mol. Med. (2024) https://doi.org/10.1038/s12276-024-01224-z.

[7] T. Kim, C.M. Croce, MicroRNA: trends in clinical trials of cancer diagnosis and therapy strategies, Exp. Mol. Med. 55 (2023) 1314–1321, https://doi.org/10.1038/s12276-023-01050-9.

[8] Y. Xing, G. Ruan, H. Ni, H. Qin, S. Chen, X. Gu, J. Shang, Y. Zhou, X. Tao, L. Zheng, Tumor immune microenvironment and its related miRNAs in tumor progression, Front. Immunol. 12 (2021) 624725, https://doi.org/10.3389/fimmu.2021.624725.

[9] L. Salmena, L. Poliseno, Y. Tay, L. Kats, P.P. Pandolfi, A ceRNA hypothesis: the Rosetta Stone of a hidden RNA language? Cell 146 (2011) 353–358, https://doi.org/10.1016/j.cell.2011.07.014.

[10] Y. Shi, J.B. Liu, J. Deng, D.Z. Zou, J.J. Wu, Y.H. Cao, J. Yin, Y.S. Ma, F. Da, W. Li, The role of ceRNA-mediated diagnosis and therapy in hepatocellular carcinoma, Hereditas 158 (2021) 44, https://doi.org/10.1186/s41065-021-00208-7.

[11] Y. Liu, S. Khan, L. Li, T.L.M. Ten Hagen, M. Falahati, Molecular mechanisms of thyroid cancer: a competing endogenous RNA (ceRNA) point of view, Biomedicine & pharmacotherapy = Biomedecine & pharmacotherapie 146 (2022) 112251, https://doi.org/10.1016/j.biopha.2021.112251.

[12] L. Wang, B. Li, X. Yi, X. Xiao, Q. Zheng, L. Ma, Circ_0036412 affects the proliferation and cell cycle of hepatocellular carcinoma via hedgehog signaling pathway, J. Transl. Med. 20 (2022) 154, https://doi.org/10.1186/s12967-022-03305-x.

[13] J. Li, Z.Q. Hu, S.Y. Yu, L. Mao, Z.J. Zhou, P.C. Wang, Y. Gong, S. Su, J. Zhou, J. Fan, et al., CircRPN2 inhibits aerobic glycolysis and metastasis in hepatocellular carcinoma, Cancer Res. 82 (2022) 1055–1069, https://doi.org/10.1158/0008-5472.Can-21-1259.

[14] Q.L. Jiang, S.J. Feng, Z.Y. Yang, Q. Xu, S.Z. Wang, CircHECTD1 up-regulates mucin 1 expression to accelerate hepatocellular carcinoma development by targeting microRNA-485-5p via a competing endogenous RNA mechanism, Chin. Med. J. 133 (2020) 1774–1785, https://doi.org/10.1097/cm9.0000000000000917.

[15] J. Cai, Z. Chen, J. Wang, J. Wang, X. Chen, L. Liang, M. Huang, Z. Zhang, X. Zuo, circHECTD1 facilitates glutaminolysis to promote gastric cancer progression by targeting miR-1256 and activating β-catenin/c-Myc signaling, Cell Death Dis. 10 (2019) 576, https://doi.org/10.1038/s41419-019-1814-8.

[16] M. Liu, Q. Wang, J. Shen, B.B. Yang, X. Ding, Circbank: a comprehensive database for circRNA with standard nomenclature, RNA Biol. 16 (2019) 899–905, https://doi.org/10.1080/15476286.2019.1600395.

[17] E. Clough, T. Barrett, The gene expression Omnibus database, Methods Mol. Biol. 1418 (2016) 93–110, https://doi.org/10.1007/978-1-4939-3578-9_5.

[18] H.Y. Huang, Y.C. Lin, S. Cui, Y. Huang, Y. Tang, J. Xu, J. Bao, Y. Li, J. Wen, H. Zuo, et al., miRTarBase update 2022: an informative resource for experimentally validated miRNA-target interactions, Nucleic Acids Res. 50 (2022) D222–d230, https://doi.org/10.1093/nar/gkab1079.

[19] V. Agarwal, G.W. Bell, J.W. Nam, D.P. Bartel, Predicting effective microRNA target sites in mammalian mRNAs, Elife 4 (2015), https://doi.org/10.7554/eLife.05005.

[20] P. Shannon, A. Markiel, O. Ozier, N.S. Baliga, J.T. Wang, D. Ramage, N. Amin, B. Schwikowski, T. Ideker, Cytoscape: a software environment for integrated models of biomolecular interaction networks, Genome Res. 13 (2003) 2498–2504, https://doi.org/10.1101/gr.1239303.

[21] D. Szklarczyk, A.L. Gable, K.C. Nastou, D. Lyon, R. Kirsch, S. Pyysalo, N.T. Doncheva, M. Legeay, T. Fang, P. Bork, et al., The STRING database in 2021: customizable protein-protein networks, and functional characterization of user-uploaded gene/measurement sets, Nucleic Acids Res. 49 (2021) D605–d612, https://doi.org/10.1093/nar/gkaa1074.

[22] C.J. Liu, F.F. Hu, M.X. Xia, L. Han, Q. Zhang, A.Y. Guo, GSCALite: a web server for gene set cancer analysis, Bioinformatics 34 (2018) 3771–3772, https://doi.org/10.1093/bioinformatics/bty411.

[23] B. Győrffy, Survival analysis across the entire transcriptome identifies biomarkers with the highest prognostic power in breast cancer, Comput. Struct. Biotechnol. J. 19 (2021) 4101–4109, https://doi.org/10.1016/j.csbj.2021.07.014.

[24] A.M. Newman, C.L. Liu, M.R. Green, A.J. Gentles, W. Feng, Y. Xu, C.D. Hoang, M. Diehn, A.A. Alizadeh, Robust enumeration of cell subsets from tissue expression profiles, Nat. Methods 12 (2015) 453–457, https://doi.org/10.1038/nmeth.3337.

[25] Z. Tang, C. Li, B. Kang, G. Gao, C. Li, Z. Zhang, GEPIA: a web server for cancer and normal gene expression profiling and interactive analyses, Nucleic Acids Res. 45 (2017) W98–w102, https://doi.org/10.1093/nar/gkx247.

[26] M. Li, H. Chen, L. Xia, P. Huang, Circular RNA circSP3 promotes hepatocellular carcinoma growth by sponging microRNA-198 and upregulating cyclin-dependent kinase 4, Aging 13 (2021) 18586–18605, https://doi.org/10.18632/aging.203303.

[27] Y. Huang, W. Ge, Y. Ding, L. Zhang, J. Zhou, Y. Kong, B. Cui, B. Gao, X. Qian, W. Wang, The circular RNA circSLC7A11 functions as a mir-330-3p sponge to accelerate hepatocellular carcinoma progression by regulating cyclin-dependent kinase 1 expression, Cancer Cell Int. 21 (2021) 636, https://doi.org/10.1186/s12935-021-02351-7.

[28] W. Liu, L. Zheng, R. Zhang, P. Hou, J. Wang, L. Wu, J. Li, Circ-ZEB1 promotes PIK3CA expression by silencing miR-199a-3p and affects the proliferation and apoptosis of hepatocellular carcinoma, Mol. Cancer 21 (2022) 72, https://doi.org/10.1186/s12943-022-01529-5.

[29] P. Nurse, A long twentieth century of the cell cycle and beyond, Cell 100 (2000) 71–78, https://doi.org/10.1016/s0092-8674(00)81684-0.

[30] B. Liu, G. Yang, X. Wang, J. Liu, Z. Lu, Q. Wang, B. Xu, Z. Liu, J. Li, CircBACH1 (hsa_circ_0061395) promotes hepatocellular carcinoma growth by regulating p27 repression via HuR, J. Cell. Physiol. 235 (2020) 6929–6941, https://doi.org/10.1002/jcp.29589.

[31] J.L. Duan, W. Chen, J.J. Xie, M.L. Zhang, R.C. Nie, H. Liang, J. Mei, K. Han, Z.C. Xiang, F.W. Wang, et al., A novel peptide encoded by N6-methyladenosine modified circMAP3K4 prevents apoptosis in hepatocellular carcinoma, Mol. Cancer 21 (2022) 93, https://doi.org/10.1186/s12943-022-01537-5.

[32] C. Zhu, Y. Su, L. Liu, S. Wang, Y. Liu, J. Wu, Circular RNA hsa_circ_0004277 stimulates malignant phenotype of hepatocellular carcinoma and epithelial-mesenchymal transition of peripheral cells, Front. Cell Dev. Biol. 8 (2020) 585565, https://doi.org/10.3389/fcell.2020.585565.

[33] A. Tan, Q. Li, L. Chen, CircZFR promotes hepatocellular carcinoma progression through regulating miR-3619-5p/CTNNB1 axis and activating Wnt/β-catenin pathway, Arch. Biochem. Biophys. 661 (2019) 196–202, https://doi.org/10.1016/j.abb.2018.11.020.

[34] Q. Sun, R. An, J. Li, C. Liu, M. Wang, C. Wang, Y. Wang, The role of CXCL8 and CCNB1 in predicting hepatocellular carcinoma in the context of cirrhosis: implications for early detection and immune-based therapies, J. Cancer Res. Clin. Oncol. (2023), https://doi.org/10.1007/s00432-023-05004-6.

[35] T. Zhan, X. Gao, G. Wang, F. Li, J. Shen, C. Lu, L. Xu, Y. Li, J. Zhang, Construction of novel lncRNA-miRNA-mRNA network associated with recurrence and identification of immune-related potential regulatory Axis in hepatocellular carcinoma, Front. Oncol. 11 (2021) 626663, https://doi.org/10.3389/fonc.2021.626663.

[36] C. Guo, Y. Tang, Z. Yang, G. Li, Y. Zhang, Hallmark-guided subtypes of hepatocellular carcinoma for the identification of immune-related gene classifiers in the prediction of prognosis, treatment efficacy, and drug candidates, Front. Immunol. 13 (2022) 958161, https://doi.org/10.3389/fimmu.2022.958161.

[37] S.Y. Wu, P. Liao, L.Y. Yan, Q.Y. Zhao, Z.Y. Xie, J. Dong, H.T. Sun, Correlation of MKI67 with prognosis, immune infiltration, and T cell exhaustion in hepatocellular carcinoma, BMC Gastroenterol. 21 (2021) 416, https://doi.org/10.1186/s12876-021-01984-2.

[38] C. Xue, X. Gu, Z. Bao, Y. Su, J. Lu, L. Li, The mechanism underlying the ncRNA dysregulation pattern in hepatocellular carcinoma and its tumor microenvironment, Front. Immunol. 13 (2022) 847728, https://doi.org/10.3389/fimmu.2022.847728.

[39] K. Yan, W. Cheng, X. Xu, G. Cao, Z. Ji, Y. Li, Circulating RNAs, circ_4911 and circ_4302, are novel regulators of endothelial cell function under a hepatocellular carcinoma microenvironment, Oncol. Rep. 44 (2020) 1727–1735, https://doi.org/10.3892/or.2020.7702.

[40] H. Huang, J. Peng, S. Yi, C. Ding, W. Ji, Q. Huang, S. Zeng, Circular RNA circUBE2D2 functions as an oncogenic factor in hepatocellular carcinoma sorafenib resistance and glycolysis, Am. J. Tourism Res. 13 (2021) 6076–6086.

[41] X.Y. Huang, P.F. Zhang, C.Y. Wei, R. Peng, J.C. Lu, C. Gao, J.B. Cai, X. Yang, J. Fan, A.W. Ke, et al., Circular RNA circMET drives immunosuppression and anti-PD1 therapy resistance in hepatocellular carcinoma via the miR-30-5p/snail/DPP4 axis, Mol. Cancer 19 (2020) 92, https://doi.org/10.1186/s12943-020-01213-6.

[42] J.C. Lu, P.F. Zhang, X.Y. Huang, X.J. Guo, C. Gao, H.Y. Zeng, Y.M. Zheng, S.W. Wang, J.B. Cai, Q.M. Sun, et al., Amplification of spatially isolated adenosine pathway by tumor-macrophage interaction induces anti-PD1 resistance in hepatocellular carcinoma, J. Hematol. Oncol. 14 (2021) 200, https://doi.org/10.1186/s13045-021-01207-x.